Research Article Vol. 30, No. 1 / 3 Jan 2022 / Optics Express 505
Optics EXPRESS

Diamond-based dielectric laser acceleration

TOMAS CHLOUBA,[1,*] ROY SHILOH,[1] PONTUS FORSBERG,[2] MATHIAS HAMBERG,[2] MIKAEL KARLSSON,[2] MARTIN KOZÁK,[3] AND PETER HOMMELHOFF[1]

[1]*Physics Department, Friedrich-Alexander-Universität Erlangen-Nürnberg (FAU), Staudtstraße 1, 91058 Erlangen, Germany*
[2]*Department of Materials Science and Engineering, Uppsala University, SE-751 03 Uppsala, Sweden*
[3]*Faculty of Mathematics and Physics, Charles University, Ke Karlovu 3, 12116 Prague 2, Czech Republic*
[*]*tomas.chlouba@fau.de*

Abstract: The field of dielectric laser accelerators (DLA) garnered a considerable interest in the past six years as it offers novel opportunities in accelerator science and potentially transformative applications. Currently, the most widespread approach considers silicon-based structures due to their low absorption and high refractive index in the infrared spectral region and the well-developed silicon processing technology. In this paper we investigate a diamond as an alternative to silicon, mainly due to its considerably higher damage threshold. In particular, we find that our diamond grating allows a three times higher acceleration gradient (60 MeV/m) compared to silicon gratings designed for a similar electron energy. Using more complex geometries, GeV/m acceleration gradients are within reach for subrelativistic electrons.

1. Introduction

High energy particle beams have a wide variety of applications in numerous fields, such as medicine, fundamental physics research, structural biology, food industry and coherent x-ray generation [1–4]. Most of today`s accelerators are based on radio frequency (RF) cavities whose size, power requirements and costs are rather high [5]. This has led to a considerable interest in alternative solutions. One such alternative is the now already well-known but still nascent field of dielectric laser accelerators (DLA). These are nanophotonic devices designed to accelerate particles at optical frequencies [6–10].

Currently, most of these devices [8,11–14] are based on silicon due to the highly developed industrial silicon processing, a high refractive index of ~3.45 at near infrared frequencies and relatively low absorption. However, there are several materials which may be more suitable for DLA applications. One such material is diamond. While the crystal structure of silicon is the same as that of diamond, diamond bonds are shorter and stronger, resulting in a more compact and robust material. This, in essence, also translates to a higher band gap of 5.47 eV versus 1.1 eV of silicon. A large band gap should, in principle, contribute to a high laser damage threshold, which is important in DLA as it allows for a large particle acceleration gradient. In early DLA experiments [6,7], fused silica grating structures were used, and the acceleration gradients were measured to be around 25 MV/m for subrelativistic (28 keV) electrons. For a silicon grating, the highest achieved gradient was 210 MV/m using a few-cycle laser pulse illumination, which allows for a higher peak field without inducing damage [11]. Using a more sophisticated silicon structure, still for subrelativistic electrons (96.3 keV), the highest gradient achieved is 370 MV/m over a 5.4 μm interaction length in the dual pillar silicon structure with two-sided illumination [13].

In this paper we present acceleration of electrons using a binary grating made from diamond. Additionally, we compare the damage threshold of silicon and diamond gratings and discuss the potential advantages of diamond in DLA applications.

#442752 https://doi.org/10.1364/OE.442752
Journal © 2022 Received 14 Sep 2021; revised 16 Nov 2021; accepted 19 Nov 2021; published 22 Dec 2021

Optics EXPRESS

2. Experimental setup

The diamond substrate we used was 300 µm thick with a diameter of 6 mm and consists of optical grade polycrystalline diamond from Diamond Materials in Freiburg, Germany. A thin film (160 nm) of aluminum (Al) was sputtered on the diamond. The linear grating pattern (grating period $\Lambda = 600$ nm and line width = 280 nm) was written in a 2×2 mm^2 square in a thin polymethylmethacrylate (PMMA) layer on a silicon substrate, using electron-beam lithography. The pattern was then transferred into Shipley S1813 photoresist on the Al-coated diamond using a solvent assisted micro-molding process [15]. The Al was etched in a Cl_2/BCl_3 plasma with the photoresist pattern as mask. The Al was then used as mask when etching the diamond in an oxygen and argon plasma. All etching was done in an inductively coupled plasma etcher (PlasmaTherm SLR). After etching, the mask was removed using hot piranha solution (H_2SO_4:H_2O_2, ~80 °C). Similar fabrication processes have previously been used to fabricate optical diamond gratings with longer period [16,17]. The grating depth was measured by atomic force microscopy to be 375-390 nm (which is close to the optimal depth of 400 nm based on FDTD simulations). To be able to focus the electrons above the diamond grating surface a mesa structure with the grating on top was produced (height ~50 µm and width ~40 µm) using laser ablation with a laser operating at a wavelength of 532 nm. Before laser ablation, the diamond sample was coated with molybdenum to protect the surface and avoid focusing the laser within the diamond, which may cause cracking. After the ablation, the diamond was once again cleaned in piranha solution and then placed in an oxygen plasma asher (TePla 300) for 40 min at 1000 W to remove redeposited and graphitized carbon around the laser ablated areas. The resulting structure is shown in Fig. 1.

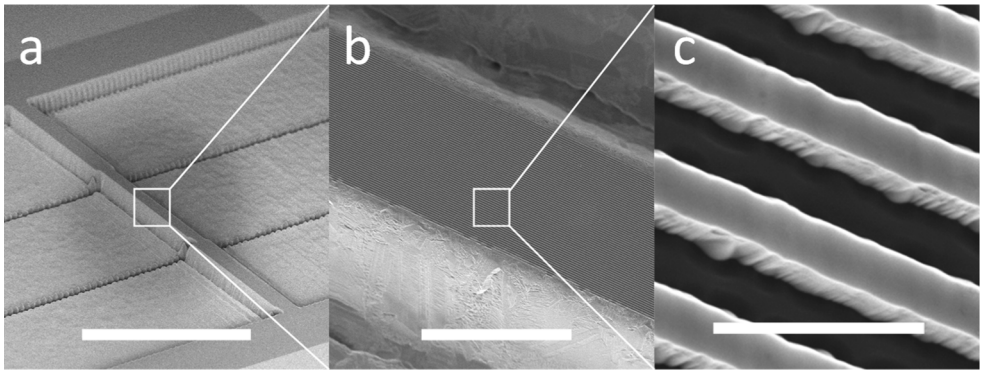

Fig. 1. SEM image of diamond gratings on mesa. White bar represents scale bars with length a) 500 µm, b) 40 µm and c) 1 µm.

The diamond grating was measured in the ultrafast scanning electron microscope (SEM), described in detail in [18]. Briefly, pulsed electrons are generated from a Schottky emitter in an XL 30 SEM illuminated by pulsed (~200 fs) UV radiation with a repetition rate of 167 kHz. These electrons are then accelerated to an energy of 26.8 keV in the SEM column. The resulting electron pulses have duration (FWHM) of about 600 fs at the DLA sample mainly due to various trajectory effects. The electron energy was chosen to satisfy the synchronicity condition for efficient acceleration, $\Lambda = \beta\,\lambda$, with Λ the diamond grating period, β the normalized electron velocity and λ the illumination wavelength. The diamond grating sample was located in the SEM chamber and illuminated by an infrared pulsed beam of 1.93 µm wavelength with a repetition rate of 167 kHz, pulse length of 680 fs and variable pulse energy and incident peak field strength. The resulting modulated electron energy was measured using a homebuilt compact magnetic spectrometer with microchannel plate (MCP) and phosphor screen (Fig. 2). The temporal delay between the electron and infrared pulses was controlled by a delay stage.

Optics EXPRESS

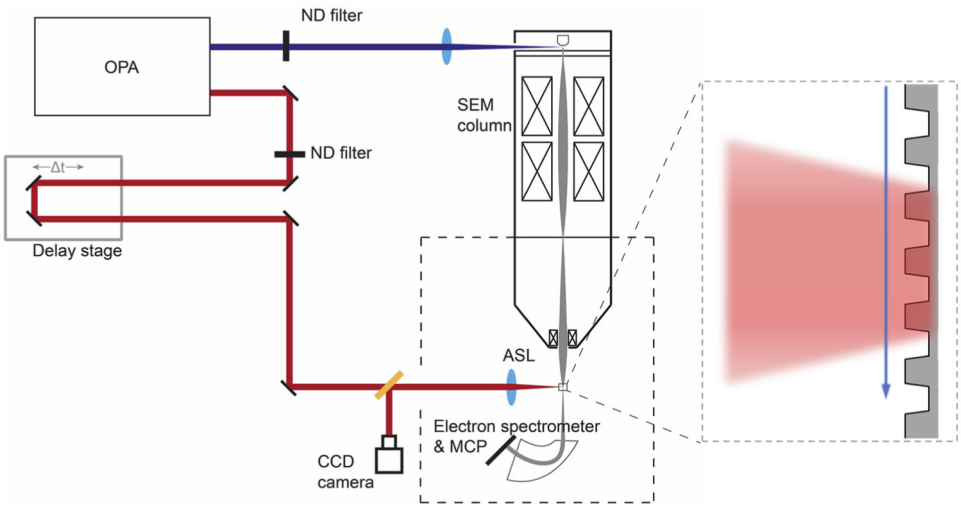

Fig. 2. A sketch of the measurement setup. UV laser pulses at 257 nm (blue line) generated from an optical parametric amplifier (OPA) trigger the electron pulses from the Schottky emitter in the SEM. Infrared laser pulses at 1.93 μm (red line) are used to illuminate the grating in the SEM chamber. Intensity of infrared illumination is controlled by a neutral density filter (ND filter) and the beam is focused onto the sample with an aspherical lens (ASL). Alignment is controlled by both SEM imaging and back-reflection of the laser from the sample to the CCD camera. The inset to the right shows a diamond grating with a blue arrow representing an electron beam. Red shading marks the incident infrared laser beam illumination.

3. Results and discussion

In Fig. 3(a) we show the measured electron energy spectrum. The spectrum (blue) was taken at maximal temporal overlap with laser pulses of 971 MV/m incident peak field and a reference spectrum (orange) was taken without laser field. Since the electron pulses were much longer than the laser optical period (6.45 fs), some electrons were accelerated and some decelerated based on which optical phase they interacted with. In order to compare the energy gain with simulations, we select the highest energy gain with at least 0.5% of the maximal electron intensity at the incident 26.8 keV energy (arrow in Fig. 3(a)). This is safely more than five times higher than the background noise, as can be clearly seen from the dashed orange curve in Fig. 3(a). We estimate the measurement uncertainty to be roughly 5% standard deviation for the incident peak field. For the energy gain measurement uncertainty we assume 10%. We plot this maximal energy gain as a function of the incident peak electric field of the incoming radiation in Fig. 3(b). The values fit very well to the predicted behavior up to an incident peak electric field of roughly 2000 MV/m. From that field strength on we observe that the data points lie below the theory curve. The energy gain starts to saturate after roughly 1500 MV/m due to dephasing: a mismatch between the optical phase and electron velocity, developed because of acceleration [14]. This effect is correctly predicted by simulation but the measured data show an even sharper decline. We strongly suspect that this decline was caused by charging effects. With increasing laser power (peak field) it became more difficult to keep the electron beam stationary relative to the grating which is typically a result of material charging. As such the measured energy gain is influenced by this as the average distance of beam from the grating was most likely larger than for previous simpler measurements due to additional fields. Finally, physical damage at high fields would manifest as a sharp decrease in the accelerated energy measured, because the phase-matching

Optics EXPRESS

condition would be violated for all electrons; however, no such drop occurred at all incident peak fields.

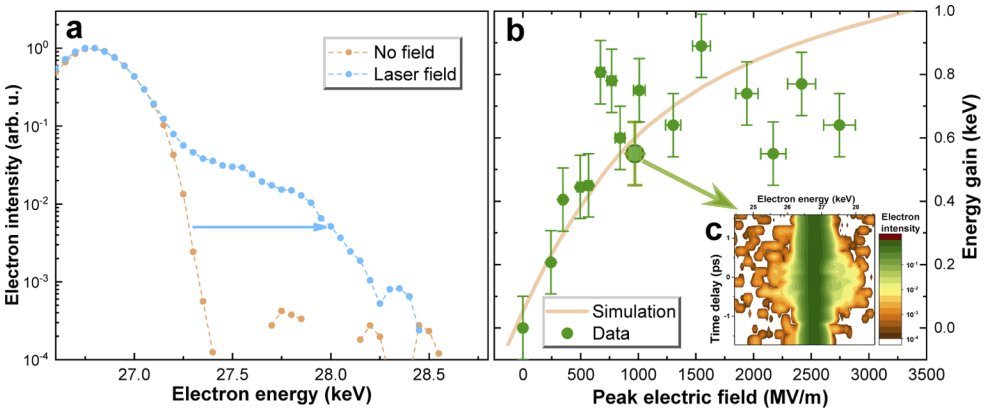

Fig. 3. a) Electron energy spectrum taken without laser field and with maximal overlap of the laser pulse (971 MV/m peak field) and electron pulse in logarithmic scale. Arrow shows the determination of maximal energy gain. b) Shows dependency of the maximal energy gain on the incident peak electric field of the laser pulse. Inset c) shows an example raw energy modulation time-delay scan in logarithmic scale for one field strength.

The electromagnetic fields were solved in 2D using the Ansys Lumerical FDTD software. In the simulation, the illumination wavelength was 1.93 μm with a Gaussian radius of 8.5 μm. The laser pulse length was set to 680 fs. The grating geometry matched the one of the experiment. The electron`s evolution through the fields obtained from the FDTD simulation was calculated using the General Particle Tracer software [19] The electron beam was simulated at different heights away from the grating, where the best agreement with measurements was found for a height of 228 nm. The calculated curve is shown as an orange line in Fig. 3(b).

The effective interaction length in the experiment between laser field and electron pulses is 15 μm, [6,13] $L_{eff} = \sqrt{\pi}\left(\frac{1}{\omega_0^2} + \frac{2\ln(2)}{(\beta c \tau_p)^2}\right)^{-1/2}$, with ω_0=8.5 μm. Therefore, the highest average gradient we achieved is 59.3 ± 6 MV/m. The measured maximal gradient is already more than double that of fused silica gratings (25 MeV/m) [6], which is also a high damage threshold material.

As evident from both experimental data and simulations, the dependence of the energy gain on the incident peak field is not linear because of the aforementioned dephasing. The simplest way to overcome this is to taper (chirp) the lattice period of the structure. This has been done [14] with silicon gratings. There, a difference between an untapered structure with an acceleration gradient of 21 MeV/m and a tapered one with gradient of 69 MeV/m was shown.

Assuming the ideal tapering, matched to the incident field where we started observing physical damage to the grating (4.74 GV/m with 250 fs pulse length), the acceleration gradient would depend linearly on the incident peak field and would reach 210 MeV/m. This is already comparable or better than single side illuminated silicon dual pillars. It has been shown [12,13] that dual pillar structures with either dual side illumination or with a distributed Bragg reflector can reach more than 10 times higher acceleration gradient than their grating predecessors. Precisely manufactured diamond dual pillars would hence reach around 2 GeV/m gradient even for subrelativistic electrons assuming the same enhancement factor. With this gradient, a subrelativistic to MeV energy accelerator can be 1 mm long or less. Naturally, the actual accelerator will be a more complex structure requiring beam confinement by APF [20–22] and prebuncher [23], so the resulting average gradient will be naturally lower.

Optics EXPRESS

One issue with diamond as a DLA material is its low electrical conductivity. Presently, mostly highly doped silicon with a resistivity between 1-5 Ω·cm is commonly used for DLAs. Any charge generated on the surface, either by multi photon excitation or by stray electrons, is then immediately transferred away. However, in undoped diamond these transient charges tend to live quite long, which may deflect electron pulses traveling close by. In our experiment, this charging issue was affecting our beam position more strongly with stronger illumination and is the probable culprit behind the mismatch between the theory curve and measured data above 2000 MV/m (Fig. 3(b)). Doping or surface treatments could alleviate this issue, but their effect on damage threshold would need to be investigated.

When subjected to femtosecond infrared laser light of sufficient intensity, the diamond lattice transforms into a graphitic one because it is thermodynamically more stable [24]. This might lower the damage threshold of diamond structures as graphite is an efficient absorber at infrared wavelengths. However, we were able to achieve acceleration gradients that were considerably higher than silicon gratings, so graphitization does not seem to be a limiting factor for employment of diamond DLA structures. A further investigation into this matter will still be needed for more complex structure geometries.

4. Conclusion

In this work we have shown that diamond grating structures represent an excellent alternative to silicon-based grating structures for DLA applications. Our measured acceleration gradient of 59.3 ± 6 MeV/m is three times higher than that of comparable silicon grating (21 MeV/m) and more than two times higher than fused silica grating (25 MeV/m). We expect to reach at least GeV/m acceleration gradients with precisely fabricated dual pillar diamond structures. Doping or surface treatments will need to be investigated to alleviate the problem of low conductivity in diamond. Since the onset of graphitization may change with a different surface structure, this will also need to be investigated using a pillar structure.

Funding. Gordon and Betty Moore Foundation (GBMF4744); European Research Council (616823, 884217); Bundesministerium für Bildung und Forschung (05K19RDE, 05K19WEB); Stiftelsen för Strategisk Forskning (ITM17-0149); Stiftelsen Olle Engkvist Byggmästare (186-0639).

Acknowledgments. Myfab is acknowledged for support and for access to the nanofabrication laboratory at Uppsala University.

Disclosures. The authors declare no conflicts of interest.

Data availability. Data underlying the results presented in this paper are not publicly available at this time but may be obtained from the authors upon request.

References

1. Focus on "Synchrotron Techniques," *Nat. Rev. Mater.* 3, 281–353 (2018).
2. P. Bucksbaum, T. Möller, and K. Ueda, "Frontiers of free-electron laser science," J. Phys. B: At. Mol. Opt. Phys. **46**(16), 160201 (2013).
3. C. J. Karzmark, "Advances in linear accelerator design for radiotherapy," Med. Phys. **11**(2), 105–128 (1984).
4. E. B. Podgorsak, *Radiation Oncology Physics: A Handbook for Teachers and Students* (International Atomic Energy Agency, 2005).
5. T. Wangler, *RF Linear Accelerators*, 2nd ed. (Wiley-VCH, 2008).
6. J. Breuer and P. Hommelhoff, "Laser-Based Acceleration of Nonrelativistic Electrons at a Dielectric Structure," Phys. Rev. Lett. **111**(13), 134803 (2013).
7. E. A. Peralta, K. Soong, R. J. England, E. R. Colby, Z. Wu, B. Montazeri, C. McGuinness, J. McNeur, K. J. Leedle, D. Walz, E. B. Sozer, B. Cowan, B. Schwartz, G. Travish, and R. L. Byer, "Demonstration of electron acceleration in a laser-driven dielectric microstructure," Nature **503**(7474), 91–94 (2013).
8. R. J. England, R. J. Noble, K. Bane, D. H. Dowell, C. K. Ng, J. E. Spencer, S. Tantawi, Z. Wu, R. L. Byer, E. Peralta, K. Soong, C. M. Chang, B. Montazeri, S. J. Wolf, B. Cowan, J. Dawson, W. Gai, P. Hommelhoff, Y. C. Huang, C. Jing, C. McGuinness, R. B. Palmer, B. Naranjo, J. Rosenzweig, G. Travish, A. Mizrahi, L. Schachter, C. Sears, G. R. Werner, and R. B. Yoder, "Dielectric laser accelerators," Rev. Mod. Phys. **86**(4), 1337–1389 (2014).
9. K. Shimoda, "Proposal for an Electron Accelerator Using an Optical Maser," Appl. Opt. **1**(1), 33 (1962).
10. A. Lohmann, "Electron acceleration by light waves," IBM Tech. Note **5**, 169–182 (1962).

Optics EXPRESS

11. M. Kozák, M. Förster, J. McNeur, N. Schönenberger, K. Leedle, H. Deng, J. S. Harris, R. L. Byer, and P. Hommelhoff, "Dielectric laser acceleration of sub-relativistic electrons by few-cycle laser pulses," Nuclear Instruments and Methods in Physics Research Section A: Accelerators, Spectrometers, Detectors and Associated Equipment **865**, 84–86 (2017).
12. P. Yousefi, N. Schönenberger, J. Mcneur, M. Kozák, U. Niedermayer, and P. Hommelhoff, "Dielectric laser electron acceleration in a dual pillar grating with a distributed Bragg reflector," Opt. Lett. **44**(6), 1520 (2019).
13. K. J. Leedle, A. Ceballos, H. Deng, O. Solgaard, R. Fabian Pease, R. L. Byer, and J. S. Harris, "Dielectric laser acceleration of sub-100 keV electrons with silicon dual-pillar grating structures," Opt. Lett. **40**(18), 4344 (2015).
14. J. McNeur, M. Kozák, N. Schönenberger, K. J. Leedle, H. Deng, A. Ceballos, H. Hoogland, A. Ruehl, I. Hartl, R. Holzwarth, O. Solgaard, J. S. Harris, R. L. Byer, and P. Hommelhoff, "Elements of a dielectric laser accelerator," Optica **5**(6), 687 (2018).
15. E. Vargas Catalan, P. Forsberg, O. Absil, and M. Karlsson, "Controlling the profile of high aspect ratio gratings in diamond," Diamond and Related Materials **63**, 60–68 (2016).
16. M. Karlsson and F. Nikolajeff, "Diamond micro-optics: microlenses and antireflection structured surfaces for the infrared spectral region," Opt. Express **11**(5), 502 (2003).
17. P. Forsberg, M. Malmström, E. V. Catalan, and M. Karlsson, "Diamond grating waveplates," Opt. Mater. Express **6**(6), 2024 (2016).
18. M. Kozák, J. McNeur, N. Schönenberger, J. Illmer, A. Li, A. Tafel, P. Yousefi, T. Eckstein, and P. Hommelhoff, "Ultrafast scanning electron microscope applied for studying the interaction between free electrons and optical near-fields of periodic nanostructures," J. Appl. Phys. **124**(2), 023104 (2018).
19. M. J. de Loos and S. B. van der Geer, *General Particle Tracer: A New 3D Code for Accelerator and Beamline Design* (n.d.).
20. U. Niedermayer, T. Egenolf, O. Boine-Frankenheim, and P. Hommelhoff, "Alternating-Phase Focusing for Dielectric-Laser Acceleration," Phys. Rev. Lett. **121**(21), 214801 (2018).
21. U. Niedermayer, T. Egenolf, and O. Boine-Frankenheim, "Three Dimensional Alternating-Phase Focusing for Dielectric-Laser Electron Accelerators," Phys. Rev. Lett. **125**(16), 164801 (2020).
22. R. Shiloh, J. Illmer, T. Chlouba, P. Yousefi, N. Schönenberger, U. Niedermayer, A. Mittelbach, and P. Hommelhoff, "Electron phase-space control in photonic chip-based particle acceleration," Nature **597**(7877), 498–502 (2021).
23. U. Niedermayer, D. S. Black, K. J. Leedle, Y. Miao, R. L. Byer, and O. Solgaard, "Low-Energy-Spread Attosecond Bunching and Coherent Electron Acceleration in Dielectric Nanostructures," Phys. Rev. Appl. **15**(2), L021002 (2021).
24. V. V. Kononenko, V. M. Gololobov, T. V. Kononenko, and V. I. Konov, "Photoinduced graphitization of diamond," Laser Phys. Lett. **12**(1), 016101 (2015).